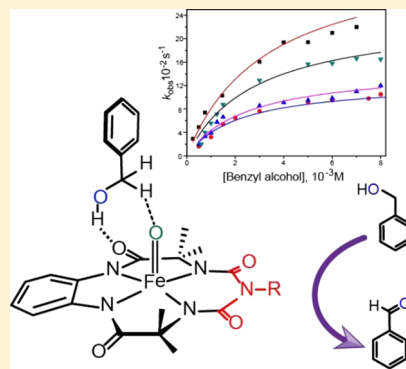


Mechanism of Alcohol Oxidation by Fe^V(O) at Room TemperatureMunmun Ghosh,^{†,§} Y. L. K. Nikhil,^{§,†} Basab B. Dhar,[‡] and Sayam Sen Gupta^{*,†}[†]Chemical Engineering Division, CSIR-National Chemical Laboratory, Pune 411008, India[‡]Department of Chemistry, Shiv Nadar University, Goutam Buddha Nagar, UP 201314, India

Supporting Information

ABSTRACT: Selective oxidation of alcohol to its corresponding carbonyl compound is an important chemical process in biological as well as industrial reactions. The heme containing enzyme CytP450 has been known to selectively oxidize alcohols to their corresponding carbonyl compounds. The mechanism of this reaction, which involves high-valent Fe^{IV}(O)–porphyrin^{•+} intermediate with alcohol, has been well-studied extensively both with the native enzyme and with model complexes. In this paper, we report for the first time the mechanistic insight of alcohol oxidation with Fe^V(O) complex of biuret TAML (bTAML), which is isoelectronic with Fe^{IV}(O)–porphyrin^{•+} intermediate form in CytP450. The oxidations displayed saturation kinetics, which allowed us to determine both the binding constants and first-order rate constants for the reaction. The *K* and *k* values observed for the oxidation of benzyl alcohol by Fe^V(O) at room temperature (*K* = 300 M⁻¹, *k* = 0.35 s⁻¹) is very similar to that obtained by CytP450 compound I at -50 °C (*K* = 214 M⁻¹, *k* = 0.48 s⁻¹). Thermodynamic parameters determined from van't Hoff's plot ($\Delta H \sim -4$ kcal/mol)

suggest hydrogen bonding interaction between substrate and bTAML ligand framework of the Fe^V(O) complex. Analysis of H/D KIE (*k_H*/*k_D* ~ 19 at 303 K), Hammett correlation and linearity in Bell-Evans-Polyanski plot points to the C–H abstraction as the rate determination step. Finally, experiments using Fe^V(O¹⁸) for benzyl alcohol oxidation and use of the “radical clock” cyclobutanol as a substrate shows the absence of a rebound mechanism as is observed for CytP450. Instead, an ET/PT process is proposed after C–H abstraction leading to formation of the aldehyde, similar to what has been proposed for the heme and nonheme model compounds.

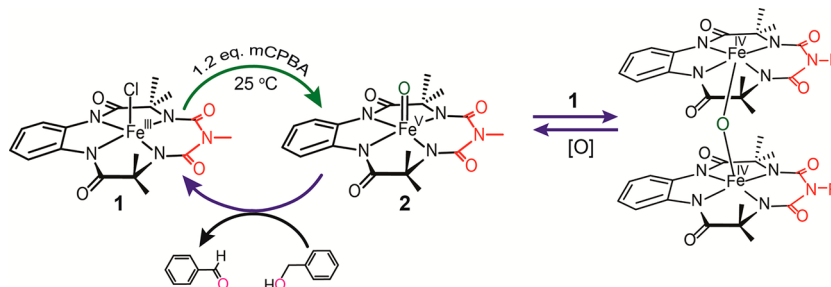


INTRODUCTION

High valent iron oxo species of heme and nonheme containing monooxygenase are invoked as reactive intermediates for the catalytic oxidation of organic substrates in numerous biological processes.^{1–5} For heme containing enzymes such as cytochrome P450 (CytP450), the Fe^{IV}(O)–porphyrin^{•+} is an active oxidant, which catalyzes alkane hydroxylation, olefin epoxidation, and alcohol oxidation.^{6–9} In the nonheme family of enzymes, both Fe^{IV}(O) and Fe^V(O) have been frequently proposed as the reactive intermediates for the oxidation of organic substrates. The reactivity landscape of both Fe^{IV}(O)– and nonheme Fe^{IV}(O)–porphyrin^{•+} toward oxidation of several organic substrates like alkanes, alkenes, and alcohols have been explored in detail.^{10–15} In contrast, reports on the reactivity of Fe^V(O) toward organic substrates, an intermediate proposed for Rieske dioxygenase family, are scarce.^{16–20} We have recently reported the formation of bTAML-Fe^V(O) of Fe^{III}-bTAML at room temperature that has been characterized by several spectroscopic techniques.²¹ The reactivity of Fe^V(O) using bTAML and TAML ligands toward oxidation of C–H bonds in alkanes, C=C bonds in alkenes, and sulphoxidation has been recently reported by us and others.^{18,19,21–24} Oxidation of alcohol to the corresponding carbonyl compound is an important chemical process in biological as well as industrial reactions.^{25–27} Hence understanding the mechanism of this process is very important in our quest not only to

understand biological oxidation but also to develop bioinspired catalysts for environmentally benign catalysis. Mechanism of alcohol oxidation with CytP450 has been evaluated under both catalytic and single turnover conditions.^{28,29} The proposed mechanism consisted of the following steps: (i) binding of benzyl alcohol to the enzyme, (ii) α -CH abstraction from benzyl alcohol, (iii) rebound of the –OH from Fe^{IV}(OH) heme, and (iv) dehydration of the gem-diol to form an aldehyde. Single turnover experiments performed with quantitative generation of CytP450 compound I at -50 °C afforded a binding constant of 214 M⁻¹ and a first-order rate constant of 0.48 s⁻¹ corresponding to the C–H abstraction.²⁸ In contrast, alcohol oxidation with model compounds containing the Fe^{IV}(O)–porphyrin^{•+} and nonheme Fe^{IV}(O) displayed no binding of the substrate to the Fe(O) intermediates. In addition, instead of a “rebound” mechanism, the oxidation was shown to proceed by a two-electron oxidation process.³⁰ Herein, we provide the first report for the mechanistic insights into alcohol oxidation by an in situ generated bTAML Fe^V(O) at room temperature. We show that similar to compound I studies, binding of the benzyl alcohol to the bTAML Fe^V(O) occurs with binding constants of ~300 M⁻¹. However, the mechanism of oxidation involves a two-

Received: August 25, 2015

Scheme 1. Schematic Representation for Benzyl Alcohol Oxidation by Fe^V(O)

electron process similar to what has been observed for the heme and nonheme model compounds.³⁰

EXPERIMENTAL SECTION

Materials. Fe–bTAML (1) was synthesized by our previously reported method.³¹ Meta-chloroperbenzoic acid (*m*CPBA, Aldrich 77%) was purified by an established method. Acetonitrile (HPLC grade, Aldrich) was used passing through an activated neutral alumina column and then dried as described elsewhere. ¹⁸O-enriched water (98%) was procured from the Shanghai Research Institute of Chemical Industry (China). Benzyl alcohol (Aldrich, 99.8%) was passed through activated neutral alumina and distilled prior to use. All reactions were carried out without any special precautions under atmospheric conditions unless otherwise specified.

General Instrumentation. UV–vis spectral studies were carried out using an Agilent diode array 8453 spectrophotometer with an attached electrically controlled thermostat. Gas chromatography (GC) was performed on a PerkinElmer Arnel Clarus 500 instrument equipped with a hydrogen flame ionization detector; HP5 columns (polar) (12 m × 0.32 mm × 1.0 μm) were used with helium as the carrier gas at a flow rate of 1 mL min⁻¹. GC-MS was performed on an Agilent 5977A mass selective detector interface with an Agilent 7890B gas chromatograph using a HP-5 ms capillary column (30 m × 0.32 mm × 0.25 μm, J&W Scientific). HR-MS was performed in a Thermo Scientific Q-Exactive Orbitrap analyzer using an electrospray ionization source connected with a C18 column (150 m × 4.6 mm × 8.0 μm).

Reactivity of Fe^V(O) (2) toward Benzyl Alcohol Oxidation. Triplicate kinetic runs were carried out for each experiment, and mean values are reported here. The kinetics were monitored in either the kinetic mode of the spectrophotometer or the scanning spectral kinetics mode using a 1.0 cm quartz cell at 399 nm (Isosbestic points of Fe^{IV} species and Fe^{III}) at 25 °C. All kinetic experiments were carried out in CH₃CN. During kinetic measurements, Fe^V(O) was generated by adding 1.2 equiv of *m*CPBA and then substrate was added to it under pseudo-first order conditions. (Concentration of 2 was from 2 × 10⁻⁵ to 1 × 10⁻⁴ M, depending upon reactivity of the substrate, and different benzyl alcohol concentrations were chosen according to the experiment, which were from 2 × 10⁻⁴ to 1.8 × 10⁻¹ M.) Pseudo-first-order rate constant (*k*_{obs}) was calculated at the isosbestic wavelength by using a nonlinear curve fitting [*A*_t = *A*_α - (*A*_α - *A*₀)e^(-*k*_{obs}*t*)] and had good agreement in rate constant value within 10% error.

Single-Turnover Reaction. Excess substrate (20 equiv. 1 × 10⁻³ M) was added to a freshly prepared 500 μL solution of 2 [generated by reaction of 1 (5 × 10⁻⁵ M) and *m*CPBA (6 × 10⁻⁵ M)] at room temperature (RT)]. Reaction mixture was stirred for 2–3 min. After completion of the reaction (determined by UV–vis spectroscopy), the products (yield %) were quantified by GC using a calibration curve obtained with authentic benzaldehyde of respective benzyl alcohol. The products were identified by GC-MS.

¹⁸O Incorporation Experiment. To 200 μL of an acetonitrile solution of 1 (5 × 10⁻⁵ M), 1.2 equiv of *m*CPBA was added, which leads to the formation of Fe^V(O) (2). H₂O¹⁸ (20 μL) was introduced into the solvent media of species 2, and the solution was allowed to stand at -22 °C for approximately 3 h. The HRMS showed 70% incorporation of O¹⁸ leading to the formation of [Fe^V(O¹⁸)

(bTAML)] *m/z* 431.0763 (calculated *m/z* 431.0773) as previously reported.²¹ Twenty microliters of a benzyl alcohol solution of 10⁻¹ M benzyl alcohol was added to the labeled Fe^V(O¹⁸) solution and immediately checked the GC-MS.

RESULTS AND DISCUSSIONS

Kinetics of Benzyl Alcohol Oxidation. Fe^V(O) was generated at 25 °C from the parent bTAML activator, (Et₄N)₂[Fe^{III}(Cl)-(bTAML)] (1), in CH₃CN by adding equimolar (1.2 equiv) amounts of *m*cpba, as reported before.²¹ The unprecedented stability²¹ of 2 at RT allowed us to perform extensive kinetic studies under single-turnover conditions to ascertain the mechanism of benzyl alcohol oxidation by Fe^V(O) using UV–vis spectroscopy. Upon addition of benzyl alcohol (20 equiv. 10⁻³ M) to a solution of 2 (5 × 10⁻⁵ M), the green color of the reaction mixture immediately changed to violet. This is ascribed to the formation of the μ-oxo-Fe^{IV} dimer which has been characterized earlier by UV–vis spectroscopy and NMR.²¹ Although the two electron oxidation of alcohol to aldehyde is expected to reduce Fe^V species to parent Fe^{III} complex 1, the fast comproportionation reaction between 1 and 2 (eq 2, 1.0 × 10⁵ M⁻¹ s⁻¹); much faster than the rate of alcohol oxidation²¹ leads to the formation of the μ-oxo-Fe^{IV} dimer. This Fe^{IV} species slowly regenerates back to the parent Fe^{III} complex quantitatively over time (Figure 1).

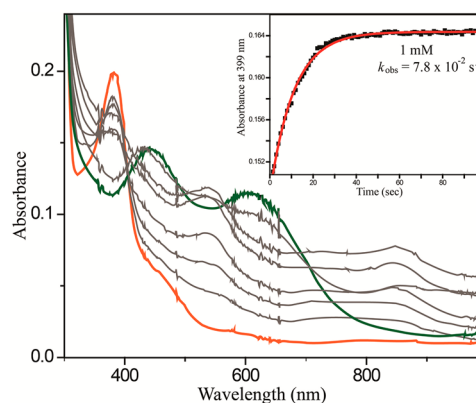
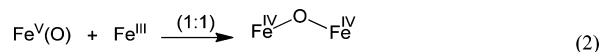
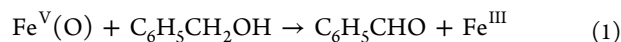


Figure 1. UV–vis spectral changes upon reaction of 2 (5 × 10⁻⁵ M) with 1 mM of benzyl alcohol. (Inset) Absorbance vs time plot at 399 nm. Red line is the first-order fit according to the equation *A*_t = *A*_α - (*A*_α - *A*₀)e^(-*k*_{obs}*t*).

The pseudo-first-order rate constant (k_{obs}), measured at the isobestic point of Fe^{III} and Fe^{IV} , correlated linearly with the substrate concentration when the substrate concentration was varied between 0.25 to 1.0 mM. The slope of the straight line provided us the second-order rate constant k_2 of $75 \pm 10 \text{ M}^{-1} \text{ s}^{-1}$ (Figure SI 1). After completion of the reaction, benzaldehyde was identified as the sole product ($\sim 72\%$) and no further oxidation to benzoic acid was observed. On the basis of the fast comproportionation between **1** and **2**, only 50% yield of the benzaldehyde is expected upon reaction of **2** with alcohol (Figure SI 2). The higher yields of benzaldehyde ($\sim 72\%$) observed are due to the subsequent reaction of alcohol with the μ -oxo- Fe^{IV} dimer (Figure 8; reaction discussed later; Figure SI 3). Similarly, second-order rate constants of different-substituted benzyl alcohols were calculated (Figure SI 4–6).

When the single turnover experiments were performed at higher concentration of alcohol ($>1 \text{ mM}$, 30 equiv), saturation behavior of the pseudo-first-order rate constant (k_{obs}) was observed for benzyl alcohol and its substituents (Figure 2 and

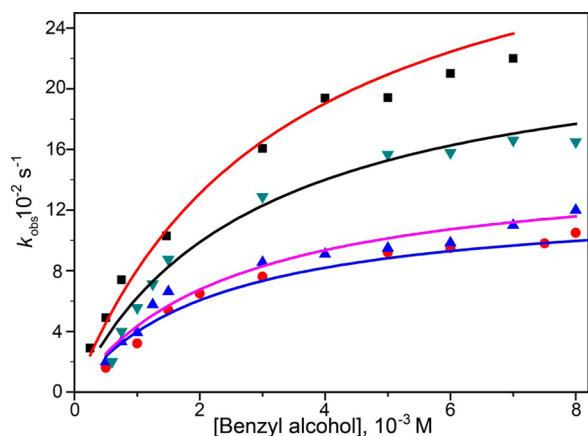
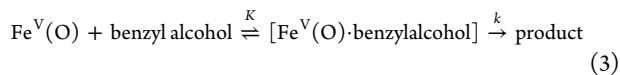


Figure 2. Pseudo-first-order kinetic analysis for the oxidation of benzyl alcohol at 300 K (red), 293 K (black), 288 K (pink), and 283 K (blue).

Figure SI 7). This points to the existence of a pre-equilibrium process before the oxidation reaction.³² It is suggesting a noncovalent interaction between $\text{Fe}^{\text{V}}(\text{O})$ and benzyl alcohol leading to an intermediate formation. Taking into account the pre-equilibrium process (eq 3), the k_{obs} obtained was plotted against different concentration of benzyl alcohol. Fitting k_{obs} to concentration of the substrate using saturation rate law (4) gave the equilibrium constants (K) of the pre-equilibrium processes and the rate constants (k) of the subsequent oxidation reactions.



$$k_{\text{obs}} = \frac{kK[\text{benzyl alcohol}]}{1 + K[\text{benzyl alcohol}]} \quad (4)$$

The equilibrium constant K_{300} , the rate constant k_{300} at 300 K, was determined to be $300 \pm 25 \text{ M}^{-1}$ at 300 K and $0.35 \pm 0.05 \text{ s}^{-1}$, respectively. Consistent with this analysis, the product, $K_{300} \times k_{300}$ ($104.7 \text{ M}^{-1} \text{ s}^{-1}$) is equal within error to the value of k_2 measured at lower benzyl alcohol concentrations ($80 \pm 10 \text{ M}^{-1} \text{ s}^{-1}$). The large equilibrium constant values indicate strong binding interaction between **2** and benzyl alcohol during the course of the reaction. The K and k values we have observed are

very similar to those obtained for the oxidation of benzyl alcohol by CytP450 compound I at $-50 \text{ }^\circ\text{C}$ ($K = 214 \text{ M}^{-1}$, $k = 0.48 \text{ s}^{-1}$).²⁸ Likewise, equilibrium constants (K) and rate constants (k) of different substituted benzyl alcohols were also calculated (SI Table). For model compounds, binding of alcohol to metal-oxo has been recently reported for the oxidation of alcohols by $\text{Ru}^{\text{IV}} = \text{O}$ complex in water where an equilibrium constant of $92 \pm 6 \text{ M}^{-1}$ was obtained at 280 K.³³ To determine the thermodynamic parameters for the pre-equilibrium process and the subsequent oxidation reaction, the oxidation of benzyl alcohol by **2** were carried out at different temperatures, and all the values of K and k are summarized in Table 1. The plots of the equilibrium constants K and the rate

Table 1. Equilibrium Constants and Rate Constants at Different Temperatures Determined in the Oxidation of Benzyl Alcohol by bTAML- $\text{Fe}^{\text{V}}(\text{O})$ Complex from Equation 4

temperature (K)	equilibrium constant K (M^{-1})	rate constant k (s^{-1})
300	300 ± 25	0.35
293	350 ± 25	0.24
288	405 ± 15	0.15
283	454 ± 28	0.12

constants k relative to the inverse of the reaction temperatures T^{-1} (Eyring plots and van't Hoff plots, respectively; Figure 3, panels A and B) allowed us to obtain the thermodynamic parameters for the pre-equilibrium processes and the activation parameters for the alcohol oxidation, respectively. As indicated by the thermodynamic parameters from the van't Hoff's plot, the formation of the precursor complex is exothermic and the value of $\sim 4 \text{ kcal/mol}$ suggests hydrogen-bonding interaction between substrates and bTAML ligand framework of $\text{Fe}^{\text{V}}(\text{O})$. This is quite reasonable since the bTAML ligand framework has four carbonyl oxygen close to the $\text{Fe}^{\text{V}}(\text{O})$ in the ligand moiety, and these are capable of forming H-bonds with the alcohol (Figure 9). The activity parameters obtained from the Eyring plot ($\Delta H^\ddagger = 10 \text{ kcal mol}^{-1}$; $\Delta S^\ddagger = -26 \text{ cal mol}^{-1} \text{ K}^{-1}$) are indicative of a well-organized transition state (Table 2). These are also extremely similar to the activation parameters for CytP450 compound I ($\Delta H^\ddagger = 13.2 \text{ kcal mol}^{-1}$) and $\text{Fe}^{\text{IV}}(\text{O})$ radical cation of electron-rich porphyrins ($\Delta H^\ddagger = 9.6 \text{ kcal mol}^{-1}$; $\Delta S^\ddagger = -26 \text{ cal mol}^{-1} \text{ K}^{-1}$) described earlier.²⁸ This is expected since the $\text{Fe}^{\text{IV}}(\text{O})$ radical cation is isoelectronic with the $\text{Fe}^{\text{V}}(\text{O})$ of our complex. However, for model heme-systems, no binding of the substrate to the complex is reported. In addition, no saturation behavior was observed for toluene oxidation (0.1 M, 1000 equiv) by $\text{Fe}^{\text{V}}(\text{O})$ (second-order rate constant $k_2 = 0.136 \text{ M}^{-1} \text{ s}^{-1}$) that we reported earlier.²¹ This leads us to speculate that the amide oxygens allow H-bonding to form an adduct of bTAML- $\text{Fe}^{\text{V}}(\text{O})$ with benzyl alcohol.

To probe the generality of these observations, the oxidation of cyclohexanol ($>100 \text{ equiv}$, 5 mM) with $\text{Fe}^{\text{V}}(\text{O})$ **2** ($5 \times 10^{-5} \text{ M}$) was also studied under single turnover conditions. As with benzyl alcohol, saturation behavior of the pseudo-first-order rate constant k_{obs} was observed (Figure SI 8). Fitting k_{obs} to concentration of the substrate using saturation rate law (3) gave the equilibrium constants of the pre-equilibrium processes ($K = 77 \pm 3 \text{ M}^{-1}$) and the rate constants of the subsequent oxidation reactions ($k = 0.19 \pm 0.023 \text{ s}^{-1}$). The rate constant k for cyclohexanol was determined to be pertinently slower (0.19 s^{-1} at 298 K) than benzyl alcohol. The equilibrium constant of the

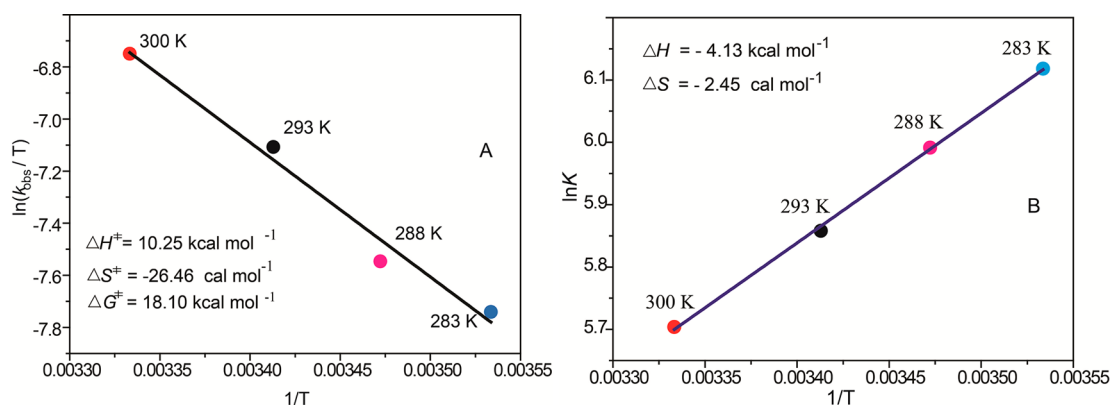


Figure 3. (A) Eyring plot. (B) van't Hoff plots for oxidation of benzyl alcohol with a $\text{Fe}^{\text{V}}(\text{O})$ complex.

Table 2. Thermodynamic Parameters Obtained from Eyring and van't Hoff Plot

ΔH [kcal mol ⁻¹]	-4.13 ± 0.3	ΔH^\ddagger [kcal mol ⁻¹]	$+10.25 \pm 0.8$
ΔS [cal K ⁻¹ mol ⁻¹]	-2.45 ± 0.5	ΔS^\ddagger [cal K ⁻¹ mol ⁻¹]	-26.46 ± 1.2

pre-equilibrium binding was less than that observed for benzyl alcohol. This is expected since benzyl alcohol has a lower $\text{p}K_{\text{a}}$ than cyclohexanol (16 compared to 15.4) and hence is expected to form stronger H bonds. Also, the conformational flexibility of the $-\text{OH}$ group in cyclohexanol is lower than benzyl alcohol. We anticipated that the $-\text{OH}$ in the benzyl alcohol or in cyclohexanol is responsible for the pre-equilibrium process resulting in an ordered transition state during the oxidation reaction.

Mechanistic Study for the Oxidation of Benzyl Alcohol. In order to obtain a mechanistic picture for the oxidation process, several experiments were performed. This includes determination of kinetic isotope effect (KIE) of C–H abstraction, linear free energy relationship (LFRE) with substituted benzyl alcohols, experiments using $\text{Fe}^{\text{V}}(\text{O}^{18})$, and oxidation of cyclobutanol as a radical clock.

Kinetic Isotope Effect. The kinetics of benzyl alcohol with high valent $\text{Fe}^{\text{V}}(\text{O})$ (5×10^{-5} M) species were studied using (*d*₂)-benzyl alcohol ($\text{C}_6\text{H}_5-\text{CD}_2\text{OH}$) as the substrate (1.5–3 mM) to determine the kinetic isotope effect ($k_{\text{H}}/k_{\text{D}}$). A very large KIE value of 19 ± 2 was determined at 30 °C. Such nonclassical large H/D KIE values (>7), observed for Fe^{IV} intermediates in enzymes such as methane monooxygenase³⁴ or TaUD oxoiron intermediates³⁵ has been ascribed to a hydrogen atom tunnelling reaction. For oxidation of benzyl alcohol by CytP450 compound I, $k_{\text{H}}/k_{\text{D}}$ has been determined 28 ± 2 at 23 °C.³⁶

In order to determine if tunnelling was taking place, the temperature-dependent second-order rate constants of benzyl alcohol and (*d*₂)-benzyl alcohol were performed between 30 °C and -10 °C. There are three key criteria for determining tunneling effects in terms of the Arrhenius equation as has been described by Bell.³⁷ These include (i) the KIE $k_{\text{H}}/k_{\text{D}} > 7$ and is temperature dependent; (ii) the ratio $A_{\text{H}}/A_{\text{D}} < 0.7$, where A is the pre-exponential term in the Arrhenius equation, and (iii) a difference in activation energy (ΔE_{a}) between C–H and C–D substrates greater than the ZPE difference of 1.13 kcal mol⁻¹. We observe that for benzyl alcohol oxidation, the KIE increases with decreasing temperature (Table 3). The Arrhenius pre-exponential factor ($\ln A_{\text{H}}$) and activation energy E_{a} were determined to be 15 and 6.6 kcal/mol (Figure 4). For the (*d*₂)-

Table 3. Second-Order Rate Constant of $\text{C}_6\text{H}_5\text{CH}_2\text{OH}$ (k_{H}) and $\text{C}_6\text{H}_5\text{CD}_2\text{OH}$ (k_{D}) at Different Temperatures and Corresponding KIE

temperature (K)	k_{H} (M ⁻¹ s ⁻¹)	k_{D} (M ⁻¹ s ⁻¹)	KIE
303	75 ± 10	4 ± 0.54	19 ± 2
283	62 ± 7	2 ± 0.4	25 ± 3
273	33 ± 7	1 ± 0.02	33 ± 4
263	14 ± 3	0.25	54 ± 7

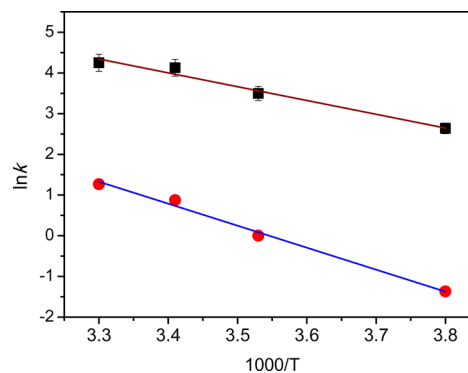


Figure 4. Plot of $\ln k$ vs $1000/T$ (Arrhenius plot) of $\text{C}_6\text{H}_5\text{CH}_2\text{OH}$ (brown line) and $\text{C}_6\text{H}_5\text{CD}_2\text{OH}$ (blue line).

benzyl alcohol, these two values ($\ln A_{\text{D}}$ and E_{a}) were determined to be 19.2 and 10.7 kcal/mol, respectively. This corresponds to $A_{\text{H}}/A_{\text{D}} = 0.025$ and $\Delta E_{\text{a}} = 4.1$ kcal/mol. Both these values suggest the presence of a tunnelling effect.

All the above data indicates that the activation of alcohols occurs exclusively by hydrogen atom abstraction from the α -CH of benzyl alcohol, and that C–H bond cleavage is the rate-determining step in the alcohol oxidation. The large negative enthalpy value and well-organized transition state observed from the activation parameters discussed above agree well with the high nonclassical KIE.

Linear Free Energy Relationship. Oxidation of various *p*-substituted benzyl alcohol (0.25–1.50 mM) by $\text{Fe}^{\text{V}}(\text{O})$ (5×10^{-5} M) was also studied to validate if hydrogen atom abstraction from the α -CH of benzyl alcohol represented the rate-determining step. From eq 4, the equilibrium constant values (K) for various substituted alcohols were determined to be 300 ± 60 M⁻¹ (SI Table). This connotes that para-substituents on benzyl alcohol have very little or no effect on the pre-equilibrium process. The k_{rel} ($k_{\text{rel}} = k_{\text{X}}/k_{\text{H}}$) value for benzyl alcohol and its analogue was plotted against the

Hammett parameter, and ρ value -0.67 was obtained from the slope (Figure 5). The relatively small value of ρ indicates that

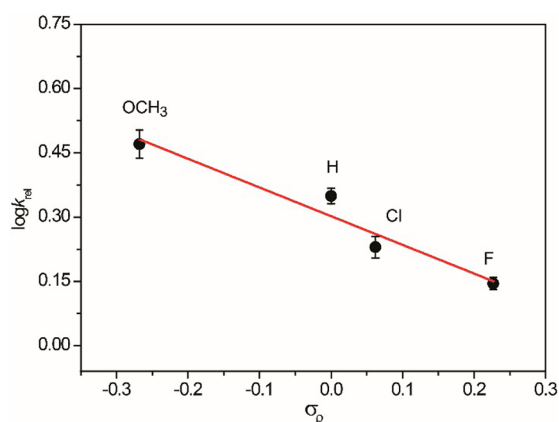


Figure 5. Hammett plot of $\log k_{rel}$ against substituent constants of benzyl alcohols.

consistent with the mechanism proposed on the basis of KIE, the reaction rates are not greatly influenced by the electron-withdrawing and electron-donating ability of the para substituents. The Hammett value for the $\text{Fe}^{\text{V}}(\text{O})$ is slightly higher than that reported for synthetic $\text{Fe}^{\text{IV}}(\text{O})$ -porphyrin^{•+} ($\rho = -0.39$)³⁰ but lower than that obtained for the CytP450 enzymes ($\rho = -1.19$).²⁸

Further, to confirm C–H abstraction as the rate-determining step, we have plotted k_2 ($80 \text{ M}^{-1} \text{ s}^{-1}$) of benzyl alcohol (BDE = 79 kcal mol^{-1})³⁸ in the BEP graph, which was previously determined for the mechanism of alkane hydroxylation (SI 11). This plot showed a competent linear fit confirming C–H abstraction as the rate-determining step.

Oxidation with Cyclobutanol. Two possibilities exist for the carbon radical of benzyl alcohol formed after α -CH abstraction to undergo further oxidation leading to aldehyde formation. The first involves the classical “rebound mechanism” in which the $\text{Fe}^{\text{IV}}\text{–OH}$ formed upon C–H abstraction rebounds the –OH group to form a gem-diol which subsequently dehydrates to form the aldehyde. In an alternative scenario, carbon radical of benzyl alcohol can be oxidized which then transfers a H^+ to the solvent cage leading to aldehyde formation. To distinguish between the one electron and two electron process, cyclobutanol (100 equiv. 10^{-2} M) has been taken as a substrate (Figure 6).^{39,40} In this experiment upon oxidation, if ketone is

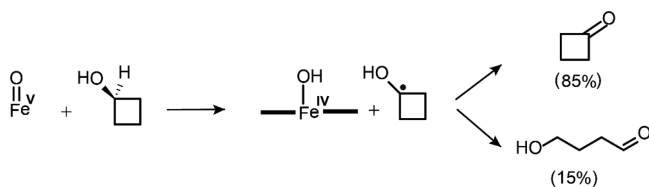


Figure 6. Oxidation of cyclobutanol by $\text{Fe}^{\text{V}}(\text{O})$ showing cyclobutanone as a major product.

the sole product then the reaction occurs by hydrogen atom abstraction followed by electron transfer. On the other hand, if a carbon radical formed by H atom abstraction of cyclobutanol and then escapes from the solvent cage, a ring open product, 4-hydroxybutanal, can be formed. Our experiment with $\text{Fe}^{\text{V}}(\text{O})$ show predominant formation of cyclobutanone

(>85%), thus indicating that the oxidation by $\text{Fe}^{\text{V}}(\text{O})$ is a two-electron process.

Oxidation Using ^{18}O labeled $\text{Fe}^{\text{V}}(\text{O})$. Oxidation of benzyl alcohol was finally carried out with an ^{18}O -labeled $\text{Fe}^{\text{V}}(\text{O})$ complex to further prove the two-electron oxidation process. Upon adding 25 equiv of benzyl alcohol (2.5 mM) to the solution of ^{18}O -labeled catalyst, only <5% of ^{18}O incorporation was observed in benzaldehyde as determined by GC-MS (overall yield of benzaldehyde >70%, Figure SI 9–10).⁴¹ If the oxidation had occurred through a two-step rebound process, a 1:1 mixture of ^{16}O - and ^{18}O -labeled benzaldehyde should have been observed. The small amount of ^{18}O incorporated product was likely the result of oxygen atom exchange between ^{16}O benzaldehyde and H_2^{18}O leading to <5% incorporation of ^{18}O in the benzaldehyde product (Figure 7). In all likelihood, the

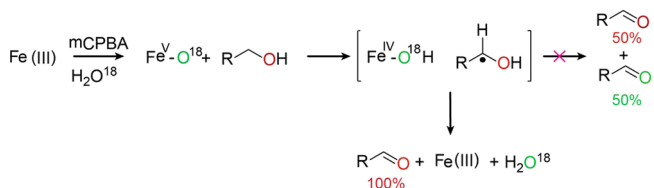


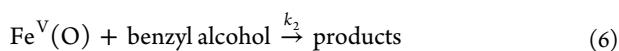
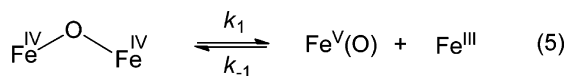
Figure 7. Benzyl alcohol oxidation with $\text{Fe}^{\text{V}}(\text{O}^{18})$, < 5% incorporation of O^{18} into benzaldehyde.

oxygen of benzyl alcohol is retained in the product benzaldehyde. This is in contrast to CytP450, where 30% ^{18}O incorporation in benzaldehyde is observed upon using $^{18}\text{O}_2$ as the oxidant, indicating a two-step rebound mechanism.²⁸ A 2-electron oxidation process similar to that observed by us has been reported for the oxidation of benzyl alcohol by both heme $\text{Fe}^{\text{IV}}(\text{O})$ radical cation and nonheme $\text{Fe}^{\text{IV}}(\text{O})$ model complexes.

Mechanistic Interpretation. To summarize the observations, the first step of alcohol oxidation by bTAML $\text{Fe}^{\text{V}}(\text{O})$ involves substrate binding with the $\text{Fe}^{\text{V}}(\text{O})$ complex (evident from the saturation kinetics). This is followed by H atom abstraction as is evidenced by very large KIE values and linearity obtained in the BEP graph (SI 11). The relatively small value of ρ obtained from the Hammett plot also supports this hypothesis. Following the H atom abstraction leading to the formation of bTAML $\text{Fe}^{\text{IV}}(\text{OH})$ and the cyclobutanol radical cage, the following possibilities exist leading to product formation: (i) diffusion of cyclobutanol radical from the cage followed by further oxidation, (ii) rapid trapping of the cyclobutanol radical via rebound to form the gem-diol, and (iii) ET/PT from the carbon radical to the $\text{Fe}^{\text{IV}}\text{–OH}$ leading to aldehyde formation. The possibility (i) is negated by the radical clock experiment using cyclobutanol, where cyclobutanone is obtained as the major product (only minor ring-opened product was observed). The ^{18}O labeling experiments which show <5% incorporation of ^{18}O in the benzaldehyde product negate the possibility of rebound (ii). We believe that $\text{Fe}^{\text{IV}}\text{–OH}$ is a strong enough oxidant ($\text{Fe}^{\text{IV}/\text{III}}$ redox potential is $\sim 0.6 \text{ V}$)⁴² to oxidize the benzyl alcohol radical via ET/PT to form the product aldehyde. Hence the likely mechanism for alcohol oxidation by bTAML $\text{Fe}^{\text{V}}(\text{O})$ involves a 2-electron process leading to a “net hydride transfer” (Figure 9).

Reactivity of μ -oxo- Fe^{IV} Dimer. The >50% yields of benzaldehyde formation observed in the single turnover experiments is unlikely because the fast comproportionation between 1 and 2 would only allow 50% of 2 to react with

benzyl alcohol and yield a maximum of only 50% benzaldehyde (with respect to **2**). The higher yields of benzaldehyde observed are due to the slow reaction of alkanes with the μ -oxo- Fe^{IV} dimer, similar to what has been observed for alkene oxidation by $\text{Fe}^{\text{V}}(\text{O})$.²² Hence the reactivity of μ -oxo- Fe^{IV} dimer with benzyl alcohol was studied at RT. The μ -oxo- Fe^{IV} dimer was generated by addition of 0.5 equiv of m-CPBA in the Fe^{III} complex. The synthesized dimer had a characteristic UV–vis spectra similar to the previously reported μ -oxo- Fe^{IV} dimer (formed in equimolar amounts of Fe^{III} and $\text{Fe}^{\text{V}}(\text{O})$; characterized by ^1H NMR and EPR).²¹ The resulting dimer species reacted with benzyl alcohol to form the corresponding benzaldehyde with rates that are ~ 200 fold slower than $\text{Fe}^{\text{V}}(\text{O})$ (Figure SI 3). Evidently, when the concentration of benzyl alcohol was increased to 1000 equiv, no saturation was observed for the k_{obs} showing that substrate-mediated disproportionation was not occurring. On the basis of prior work from our group where the epoxidation of alkenes with μ -oxo- Fe^{IV} dimer was studied,²² we hypothesized that the μ -oxo- Fe^{IV} dimer exists in an equilibrium with $\text{Fe}^{\text{V}}(\text{O})$ and Fe^{III} species and the $\text{Fe}^{\text{V}}(\text{O})$ was the species responsible for oxidation of benzyl alcohol. The reaction of benzyl alcohol with $\text{Fe}^{\text{V}}(\text{O})$ leads to more disproportionation of the dimer, leading to the formation of more $\text{Fe}^{\text{V}}(\text{O})$, which reacts with benzyl alcohol until all of it is converted back to the starting Fe^{III} complex (Figure SI 3). To prove this hypothesis, the reactions of μ -oxo- Fe^{IV} with benzyl alcohol were carried out with varying concentrations of the parent Fe^{III} complex. Reduction of reaction rates was observed with increasing concentrations of the parent Fe^{III} complex. The plot of reaction rates versus increasing concentration of Fe^{III} in the reaction mixture shows a competent fit into the kinetic model.



$$\text{rate} = \frac{k_1 k_2 [\mu\text{-oxo-Fe}^{\text{IV}}\text{dimer}][\text{benzyl alcohol}]}{k_{-1}[\text{Fe}^{\text{III}}] + k_2[\text{benzyl alcohol}]} \quad (7)$$

With the use of the second-order rate constant (k_2) that was determined earlier for benzyl alcohol oxidation using $\text{Fe}^{\text{V}}(\text{O})$, k_1 and k_{-1} were calculated under single turnover conditions using eq 7 as 0.00596 and 21833, respectively (see Figure 8). The comproportionation k_{-1} is in the error range of the value reported elsewhere independently.²¹

CONCLUSION

Oxidation of benzyl alcohol by bTAML $\text{Fe}^{\text{V}}(\text{O})$ was studied at room temperature in CH_3CN . The oxidations displayed saturation kinetics, which allowed us to determine both the binding constants and first-order rate constants for the reaction. The saturation kinetics observed are similar to the oxidation of benzyl alcohol by CytP450 compound I at -50°C under single turnover conditions.²⁸ The K and k values observed for the oxidation of benzyl alcohol by $\text{Fe}^{\text{V}}(\text{O})$ at RT ($K = 300\text{ M}^{-1}$, $k = 0.35\text{ s}^{-1}$) is very similar to that obtained by CytP450 compound I at -50°C ($K = 214\text{ M}^{-1}$, $k = 0.48\text{ s}^{-1}$). Such saturation kinetics have not been observed for model heme compound I and nonheme $\text{Fe}^{\text{IV}}(\text{O})$ reported earlier.³⁰ For oxidations of the benzyl alcohol conducted between 10 and 27°C , a van't Hoff function for binding and an Eyring function for the first-order

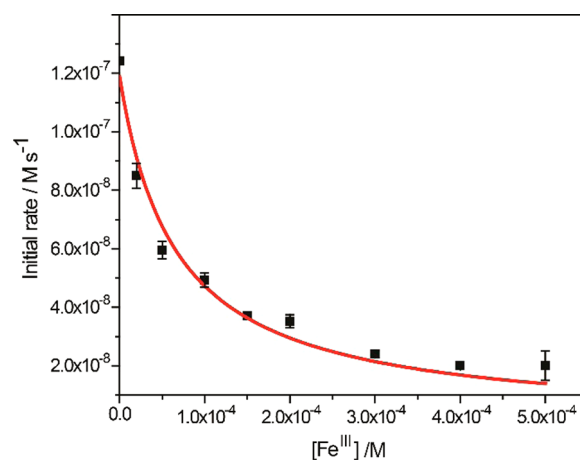


Figure 8. Plot of initial rate vs concentration of Fe^{III} , complex **1**, added for reaction of μ -oxo- Fe^{IV} dimer ($2 \times 10^{-5}\text{ M}$) with benzyl alcohol (0.015 M). k_1 (0.00596) and k_{-1} (21833) were obtained according to the nonlinear curve fit (eq 7). Reaction was performed at RT in acetonitrile solvent under air.

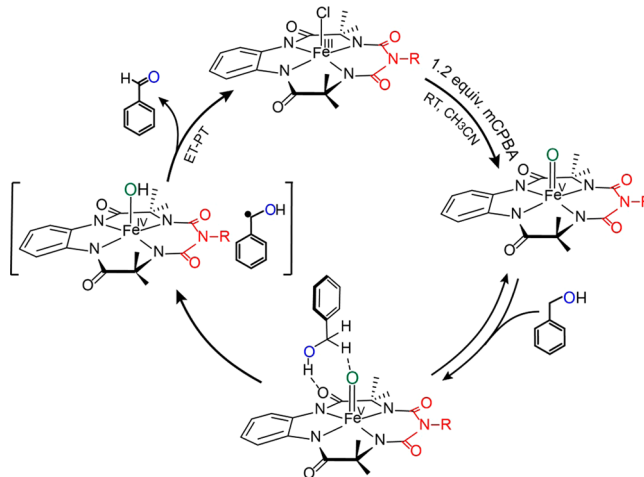


Figure 9. Proposed mechanism for alcohol oxidation with $\text{Fe}^{\text{V}}(\text{O})$.

oxidation reaction were generated. Thermodynamic parameters determined from van't Hoff's plot ($\Delta H \sim -4\text{ kcal/mol}$) suggest a hydrogen-bonding interaction between substrate and bTAML ligand framework in the $\text{Fe}^{\text{V}}(\text{O})$ complex. The first-order rate constant obtained for biuret $\text{Fe}^{\text{V}}(\text{O})$ is much smaller compared to the $\text{Fe}^{\text{IV}}(\text{O})$ radical cation of CytP450 but is comparable to the electron-rich heme model of CytP450. Analysis of H/D KIE for benzyl alcohol and its benzylic dideuterio isotopomer ($k_{\text{H}}/k_{\text{D}} \sim 19$ at 303 K), Hammett correlation with substituted benzyl alcohols and linearity in Bell-Evans-Polyanski plot points to the C–H abstraction as the rate determination step (Figure SI 11). Finally, experiments using $\text{Fe}^{\text{V}}(\text{O}^{18})$ for benzyl alcohol oxidation and use of the “radical clock” cyclobutanol as a substrate shows the absence of a rebound mechanism as is observed for CytP450. Instead, an ET/PT process is proposed after C–H abstraction, leading to formation of the aldehyde, similar to what has been proposed for the heme and nonheme model compounds. In summary, the reactivity of $\text{Fe}^{\text{V}}(\text{O})$ toward alcohol is reported for the first time. We have shown binding of substrate $-\text{OH}$ to the bTAML ligand framework of $\text{Fe}^{\text{V}}(\text{O})$. Such an interaction had not been observed earlier for model complexes. These secondary

interactions can be used to design substrates for selective oxidation of complex natural products. Work in such direction is being pursued in our laboratory.

■ ASSOCIATED CONTENT

● Supporting Information

The Supporting Information is available free of charge on the ACS Publications website at DOI: [10.1021/acs.inorgchem.5b01937](https://doi.org/10.1021/acs.inorgchem.5b01937).

Plot of k_{obs} against concentration; GC chromatogram; UV-vis spectral changes; absorbance vs time plot; plots of k_{obs} against concentration; plots of absorbance vs time; plot of k_{obs} vs substrate; table of equilibrium constant, rate constants, and second-order rate constant of substituted benzyl alcohols; GC/MS data; and $\log k'_{2}$ vs $\text{BDE}_{\text{C-H}}$ (PDF)

■ AUTHOR INFORMATION

Corresponding Author

*E-mail: ss.sengupta@ncl.res.in.

Author Contributions

§ M.G. and Y.L.K.N. contributed equally.

Notes

The authors declare no competing financial interest.

■ ACKNOWLEDGMENTS

S.S.G. acknowledges DST, New Delhi (SERB, EMR/2014/000106) for funding. M.G. acknowledge CSIR (Delhi) for fellowship. B.B.Dhar acknowledges DST, New Delhi (SERB/F/3945/2013-14) for funding.

■ REFERENCES

- Denisev, I. G.; Makris, T. M.; Sligar, S. G.; Schlichting, I. *Chem. Rev.* **2005**, *105* (6), 2253–2278.
- Costas, M.; Mehn, M. P.; Jensen, M. P.; Que, L. *Chem. Rev.* **2004**, *104* (2), 939–986.
- Groves, J. T. *Proc. Natl. Acad. Sci. U. S. A.* **2003**, *100* (7), 3569–3574.
- Que, L.; Tolman, W. B. *Nature* **2008**, *455* (7211), 333–340.
- Rittle, J.; Green, M. T. *Science* **2010**, *330* (6006), 933–937.
- Ortiz de Montellano, P. R. *Chem. Rev.* **2010**, *110* (2), 932–948.
- Shaik, S.; de Visser, S. I.; Kumar, D. *J. Biol. Inorg. Chem.* **2004**, *9* (6), 661–668.
- Pan, Z.; Newcomb, M. *Inorg. Chem.* **2007**, *46* (16), 6767–6774.
- Krest, C. M.; Onderko, E. L.; Yosca, T. H.; Calixto, J. C.; Karp, R. F.; Livada, J.; Rittle, J.; Green, M. T. *J. Biol. Chem.* **2013**, *288* (24), 17074–17081.
- Kaizer, J.; Klinker, E. J.; Oh, N. Y.; Rohde, J.-U.; Song, W. J.; Stubna, A.; Kim, J.; Münck, E.; Nam, W.; Que, L. *J. Am. Chem. Soc.* **2004**, *126* (2), 472–473.
- Bell, S. R.; Groves, J. T. *J. Am. Chem. Soc.* **2009**, *131* (28), 9640–9641.
- Han, J. H.; Yoo, S.-K.; Seo, J. S.; Hong, S. J.; Kim, S. K.; Kim, C. *Dalton Transactions* **2005**, *2*, 402–406.
- Que, L. *Acc. Chem. Res.* **2007**, *40* (7), 493–500.
- Krebs, C.; Galonicĭ Fujimori, D.; Walsh, C. T.; Bollinger, J. M. *Acc. Chem. Res.* **2007**, *40* (7), 484–492.
- Nam, W. *Acc. Chem. Res.* **2007**, *40* (7), 522–531.
- Chow, T. W.-S.; Wong, E. L.-M.; Guo, Z.; Liu, Y.; Huang, J.-S.; Che, C.-M. *J. Am. Chem. Soc.* **2010**, *132* (38), 13229–13239.
- Prat, I.; Mathieson, J. S.; Güell, M.; Ribas, X.; Luis, J. M.; Cronin, L.; Costas, M. *Nat. Chem.* **2011**, *3* (10), 788–793.
- de Oliveira, F. T.; Chanda, A.; Banerjee, D.; Shan, X.; Mondal, S.; Que, L.; Bominaar, E. L.; Münck, E.; Collins, T. J. *Science* **2007**, *315* (5813), 835–838.
- Kundu, S.; Thompson, J. V. K.; Ryabov, A. D.; Collins, T. J. *J. Am. Chem. Soc.* **2011**, *133* (46), 18546–18549.
- Chen, K.; Que, L. *J. Am. Chem. Soc.* **2001**, *123* (26), 6327–6337.
- Ghosh, M.; Singh, K. K.; Panda, C.; Weitz, A.; Hendrich, M. P.; Collins, T. J.; Dhar, B. B.; Sen Gupta, S. *J. Am. Chem. Soc.* **2014**, *136* (27), 9524–9527.
- Singh, K. K.; Tiwari, M. k.; Dhar, B. B.; Vanka, K.; Sen Gupta, S. *Inorg. Chem.* **2015**, *54* (13), 6112–6121.
- Singh, K. K.; Tiwari, M. k.; Ghosh, M.; Panda, C.; Weitz, A.; Hendrich, M. P.; Dhar, B. B.; Vanka, K.; Sen Gupta, S. *Inorg. Chem.* **2015**, *54* (4), 1535–1542.
- Kundu, S.; Thompson, J. V. K.; Shen, L. Q.; Mills, M. R.; Bominaar, E. L.; Ryabov, A. D.; Collins, T. J. *Chem.–Eur. J.* **2014**, *21* (4), 1803–1810.
- Sheldon, R. A.; Arends, I. W. C. E.; ten Brink, G.-J.; Dijkman, A. *Acc. Chem. Res.* **2002**, *35* (9), 774–781.
- Stahl, S. S. *Angew. Chem., Int. Ed.* **2004**, *43* (26), 3400–3420.
- Whittaker, J. W. *Chem. Rev.* **2003**, *103* (6), 2347–2364.
- Wang, Q.; Sheng, X.; Horner, J. H.; Newcomb, M. *J. Am. Chem. Soc.* **2009**, *131* (30), 10629–10636.
- Vaz, A. D. N.; Coon, M. J. *Biochemistry* **1994**, *33* (21), 6442–6449.
- Oh, N. Y.; Suh, Y.; Park, M. J.; Seo, M. S.; Kim, J.; Nam, W. *Angew. Chem., Int. Ed.* **2005**, *44* (27), 4235–4239.
- Panda, C.; Ghosh, M.; Panda, T.; Banerjee, R.; Sen Gupta, S. *Chem. Commun.* **2011**, *47* (28), 8016–8018.
- Mader, E. A.; Davidson, E. R.; Mayer, J. M. *J. Am. Chem. Soc.* **2007**, *129* (16), 5153–5166.
- Ohzu, S.; Ishizuka, T.; Hirai, Y.; Jiang, H.; Sakaguchi, M.; Ogura, T.; Fukuzumi, S.; Kojima, T. *Chemical Science* **2012**, *3* (12), 3421–3431.
- Nesheim, J. C.; Lipscomb, J. D. *Biochemistry* **1996**, *35* (31), 10240–10247.
- Price, J. C.; Barr, E. W.; Glass, T. E.; Krebs, C.; Bollinger, J. M. *J. Am. Chem. Soc.* **2003**, *125* (43), 13008–13009.
- Pan, Z.; Horner, J. H.; Newcomb, M. *J. Am. Chem. Soc.* **2008**, *130* (25), 7776–7777.
- Bell, R. P. *Trans. Faraday Soc.* **1959**, *55* (0), 1–4.
- Blanksby, S. J.; Ellison, G. B. *Acc. Chem. Res.* **2003**, *36* (4), 255–263.
- Pestovsky, O.; Bakac, A. *J. Am. Chem. Soc.* **2004**, *126* (42), 13757–13764.
- Rocek, J.; Radkowsky, A. E. *J. Am. Chem. Soc.* **1968**, *90* (11), 2986–2988.
- Seo, M. S.; In, J.-H.; Kim, S. O.; Oh, N. Y.; Hong, J.; Kim, J.; Que, L.; Nam, W. *Angew. Chem., Int. Ed.* **2004**, *43* (18), 2417–2420.
- Panda, C.; Debgupta, J.; Díaz Díaz, D.; Singh, K. K.; Dhar, B. B.; Sen Gupta, S. *J. Am. Chem. Soc.* **2014**, *136* (35), 12273.